



ISSN NO. 2320-5407

*Journal homepage: <http://www.journalijar.com>***INTERNATIONAL JOURNAL  
OF ADVANCED RESEARCH****RESEARCH ARTICLE****Microstructure characterization of Al-Mg alloys by X-ray diffraction line profile analysis****A.A.Akl<sup>1</sup> and A.S.Hassanien<sup>2,3</sup>****1. Faculty of Science in Ad-Dawadmi, Physics Department, Shaqra University, 11911, KSA****2. Faculty of Engineering (Shoubra), Math. and Engineering Physics Dept., Benha University, EGYPT****3. On leave to Faculty of Science in Ad-Dawadmi, Physics Dept., Shaqra University, KSA*****Manuscript Info******Manuscript History:***

Received: 19 September 2014

Final Accepted: 26 October 2014

Published Online: November 2014

***Key words:***Alloys, X-Ray diffraction,  
Deformation, dislocations,  
Microstructure**\*Corresponding Author  
Ahmed S. Hassanien*****Abstract***

Microstructure characterization of Al - Mg alloy was discussed as a function of plastic deformation degrees (0%-35.46%). The changes in the microstructure have been studied by using X-ray diffraction line profile analysis (XDLP). The lattice parameter, crystallite size, average internal stress, microstrain and dislocation density of Al-Mg alloys were calculated. Both crystallite size and microstrain were found strongly contributing in the broadening of X-ray diffraction line. The obtained results showed that, the values of the crystallite size were found to be in the range of 480-540nm and the values of the residual internal stress were found to be in the range of  $(-1.74 \times 10^9) - (-2.49 \times 10^9)$  dy/cm<sup>2</sup>. Also, the values of microstrain and dislocation density were found to be in the range of  $5.25 \times 10^{-3} - 7.75 \times 10^{-3}$  and  $3.48 \times 10^{10} - 6.18 \times 10^{10}$  line/cm<sup>2</sup>, respectively.

*Copy Right, IJAR, 2014.. All rights reserved***1. Introduction**

Since the properties of aluminum make it a valuable mineral such as light weight, durability and portability, remanufacturing and rust resistance and ease of handling and its ability to form and electrical conductivity. Due to these various characteristics of Al, there are several fields of the use of aluminum. In addition, changes in the properties of Al-Mg alloys are of key importance for a wide range of industrial applications. The properties of Al-Mg alloys such as strength and formability, can be altered by thermo-mechanical processing typically consisting of various deformation and annealing processes [1]. During deformation point defects and dislocations are introduced in the material resulting in a transformation from an ensemble of defect-free grains (Fig. 1.a) to a deformation microstructure (Fig. 1.b). The details of the microstructure depend on the material and on the deformation parameters. By a subsequent annealing new almost defect-free nuclei appear in the deformed microstructure (Fig. 1.c). Driven by the stored energy associated with the dislocations in the deformed state the new nuclei grow and invariably replace the deformed microstructure (Fig. 1.d).

These result in an overall change of the microstructure forming vacancy clusters, dislocation loops or small domains, immobile clusters of self-interstitials etc. [2,3]. The deformation induced defect clusters play a major role in governing the mechanical properties of the structural materials. The process of nucleation and growth of these new nuclei is referred to as re-crystallization. Hence, to fully control the macroscopic properties of the material, a detailed understanding of the fundamental mechanisms of deformation and annealing is required.

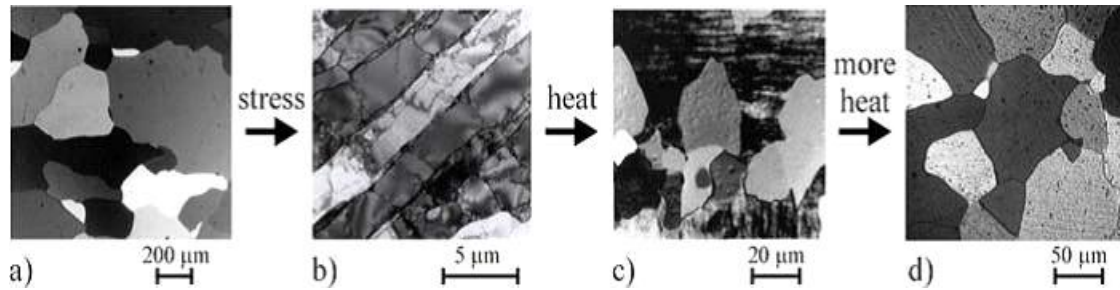


**Fig. 1: Illustration of the microstructure evolution following by deformation and annealing.**  
**Courtesy Dorte Juul Jensen.**

It is seen that the most applications and the properties of Al-Mg alloys are highly structure sensitive which in turn can severely influence the device performance. The structure parameters, the crystallinity, crystal phase, lattice constant, average internal stress and microstrain, crystallite size, orientation etc are strongly dependent on deformation percentage. The diffraction pattern obtained from a prepared sample gives information about imperfections in the material. The X-ray diffraction (XRD) peak is broadened due to small crystallite size and microstrain due to dislocations and stacking faults. The analysis of the shape of the peaks for obtaining information about the material is referred to as line profile analysis (LPA) [4-6]. The line profiles of the diffractions of various planes during XRD are characteristic of the state of the sample. The shapes of line profiles are also affected by instrument and sample shape, which is referred to as instrumental broadening. This instrumental broadening needs to be eliminated to obtain broadening exclusively due to samples effects. The observed broadening in X-ray line profiles is due to the crystallite size ( $D$ ) and microstrain, ( $\epsilon$ ) present in the Al-Mg alloys. Once the ( $D$ ) and ( $\epsilon$ ) are determined from the broadening, the dislocation density can be estimated.

Peak fitting methods are based on the analysis of the full width of the line profile at half of the maximum intensity and the integral breadth that can be easily determined from the peak profile. It is well established that profile arising due to crystallite size broadening are approximately Cauchy (Lorentzian) and due to lattice microstrain broadening is nearly Gaussian in nature. By fitting the diffraction peak profile with the Cauchy (Lorentzian) ( $\beta_C$ ) and Gaussian ( $\beta_G$ ) contributions could be determined. Alternatively,  $\beta_C$  and  $\beta_G$  of a peak are determined from the value of integral breadth and full width half maxima (FWHM) of the peak using well established relationships [7]. The domain crystallite size and lattice microstrain are calculated from corrected  $\beta_C$  and  $\beta_G$  of a peak. In the present work, we are to investigate the correlation between microstructural parameters of Al-Mg alloys and deformation degrees and discussed.

## 2. Experimental

The chemical composition of Al-Mg alloys used for the deformation process shown in Table 1. Our samples were obtained from a couple of dimensions 170x150x2.98 mm. To get samples without any thermal stresses, they were annealed at 773 Kelvin for 10 hours and then cooled to room temperature.

**Table 1: The chemical composition of the Al-Mg alloy sample**

Alloy	Si	Fe	Cu	Mn	Mg	Cr	Zn	Al
5251 Al	0.4	0.5	0.15	0.1-0.5	2.2	0.15	0.15	Reminder

The structure characteristics of the prepared samples were studied using by X-ray diffractometer (JEOL model JSDX-60PA) with attached Ni-filtered Cu-K $\alpha$  radiation ( $\lambda = 0.154184$  nm). Continuous scanning was applied with a slow scanning rate (1 $^\circ$ /min) and a small time constant (1sec). A range of  $2\theta$  (from 30 to 100 $^\circ$ ) was scanned, so that the required diffraction peaks for phase identification could be detected. XRD was performed for the phase identification and preferred orientation determination. The crystallite size and microstrain of the samples was

determined by using Williamson-Hall formula [8]. The seven diffraction planes (110), (111), (200), (220), (300), (311) and (222) characterizing the XRD patterns of the deformation samples were used for the calculation. The average values of the full-width at half-maximum (FWHM) of the characterized peaks were measured after correction of instrumental factor. Where, the pattern of the standard silicon was used to find the instrumental correction.

### 3. Results and discussion

#### 3.1. X-ray diffraction analysis

X-ray diffractograms of Al - Mg alloy samples at different degree of plastic deformation (0- 35.46 %) are shown in Fig. (2). The main features of the diffraction patterns are the same, but only a considerable variation of the peak intensity is observed. On the other hand, no peaks of free Mg were revealed. The diffraction peaks at  $2\theta = 34.7, 38.5, 44.8, 65.2, 69.5, 78.1$  and  $82.3^\circ$ , respectively, correspond to (110), (111), (200), (220), (300), (311), and (222) planes. A comparison of observed and standard (d) values for (hkl) planes as matched with standard PDF number 04-0787, indicates that the Al-Mg samples are polycrystalline and have face centered cubic structure. The increase in the intensity of the peaks may be attributed to grain growth associated with preferred orientation and/or increase in the degree of crystallinity by increasing the deformation percentage. The average value  $a_0$  of the calculated lattice parameters equals  $4.0494\text{\AA}$  in agreement with the references. However, in all cases the intensities of (111), (200) and (220) were extremely high in comparison with the other diffraction lines, indicating they are the preferential orientation of the microcrystalline.

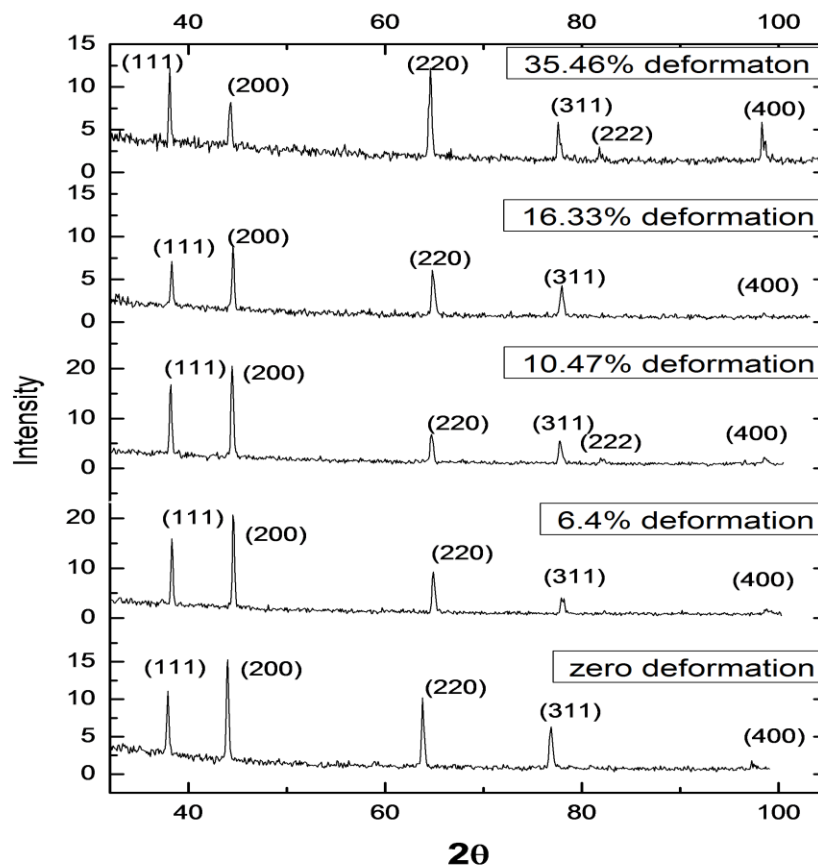
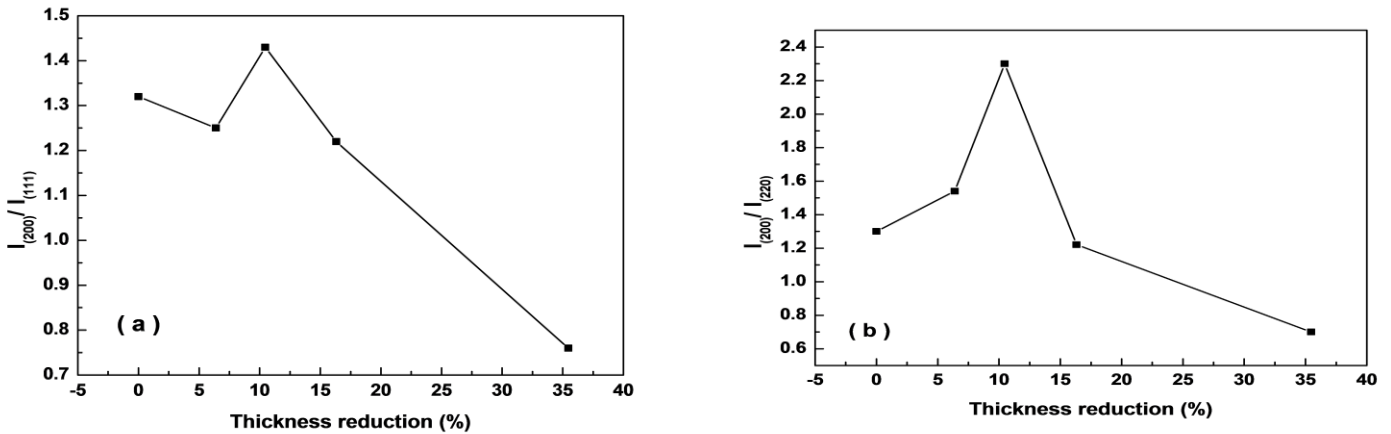


Fig. 2: X-ray diffractograms of Al-Mg alloy as a function of degree of deformation.

However, the degree of preferred orientation was found to change with the thickness reduction, this is proved on bases of the variation of the intensities ratio  $I_{(200)}/I_{(111)}$  and  $I_{(200)}/I_{(220)}$  as a function of deformation which is illustrated in Fig.(3-a and b). From these figures, it was observed that the preferred orientation is increasing to a maximum value at a deformation of 10.47% and then decreases for the higher thickness reduction. This means that, the crystallization of Al-Mg alloys is optimum at deformation percentage of 10.47%. But the decreasing of preferred orientation at higher thickness reduction is due to the agglomeration of crystals are often decomposing.



**Fig. 3: Effect of thickness reduction on: (a) a degree of preferred orientation of  $I_{(200)}/I_{(111)}$  and (b) a degree of preferred orientation of  $I_{(200)}/I_{(220)}$  of Al-Mg alloys.**

In addition, the variations of the intensities of the (111),(200),(220) and (311) peaks of Al-Mg alloys as a function of thickness reductions are shown in Fig. 4. It is clear that, the change in intensities of both the lines (111), (200), (220) and (311) are very pronounced in the deformation range of 5 - 10.47% with a maximum at 10.47%. One may conclude that, for any deformation percentage, the optimum thickness reduction is 10.47%.

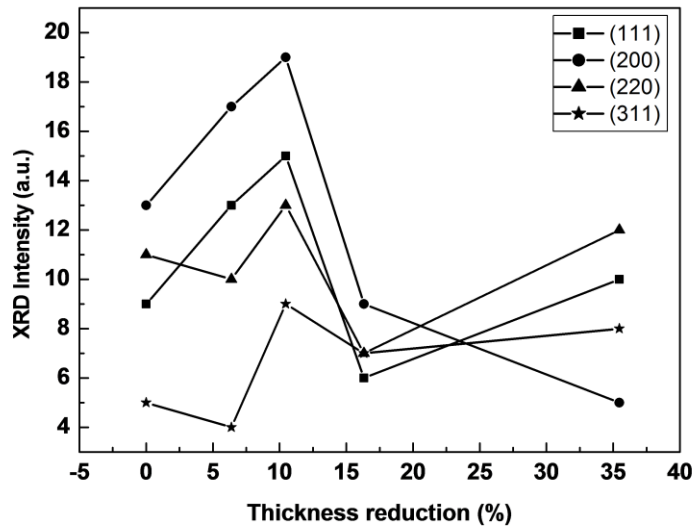


**Fig. 4: Magnitude of the X-ray diffraction intensity of the four peaks (111), (200), (220) and (311) as a function of thickness reduction of Al-Mg alloys.**

### 3.2. Determination of microstructural parameters

The basic mechanism behind the diffraction of X-ray in crystalline materials is that X-rays get scattered from crystals since their electric fields interact with the electron clouds of the atoms in the crystals. The scattered X-rays from the periodic adjacent atoms interfere and give rise to diffraction pattern. The diffraction pattern is modulated by the transfer function of the detector which in turn changes the shape of the X-ray diffraction profile. Thus a diffraction line profile is result of the convolution of a number of independent variables contributing to shape profile viz instrumental variables and microstructural effects. Instrumental variable include receiving slit width, sample transparency, the nature of the X-ray source, axial divergence of the incident beam and flat specimen geometry [9]. The microstructural effects that are responsible for the shape profile of the diffraction peaks are the finite size of the crystals or domains and the microstrain within the domain as the crystal contain lattice defects. These profiles are fitted with suitable profile shape functions in such a way that the functions must fit the asymmetric peaks and it should be mathematically as simple as possible to make the calculation of all derivatives to the variables.

#### 3.2.1. Crystallite size and microstrain

The observed integral breadth ( $B$ ) in the sample (the measurements of  $D$ ,  $\rho$  and  $\varepsilon$ ) is corrected for instrumental broadening ( $b$ ) to give corrected integral breadth ( $\beta$ ) using the following relationship [10].

$$\beta = B - \left( \frac{b^2}{B} \right) \quad (1)$$

This correction assumes that the peak shape is somewhat between Gaussian and Cauchy (Lorentzian) that leads to more exact results. The broadening in X-ray line consists of contributions due to  $D$  and  $\varepsilon$ . Following relationship is used to separate the contributions from each of them for further calculation of  $\rho$ [11].

$$\left( \frac{\beta \cos \theta}{\lambda} \right)^2 = \frac{1}{D^2} + \left( \frac{4\varepsilon \sin \theta}{\lambda} \right)^2 \quad (2)$$

Where  $\beta$  = instrumental corrected broadening (expressed in radians),  $\theta$  = Bragg's diffraction angle,  $D$  = crystallite size ( $\text{\AA}$ ),  $\varepsilon$  = microstrain and  $\lambda$  = wave length( $\text{\AA}$ ).

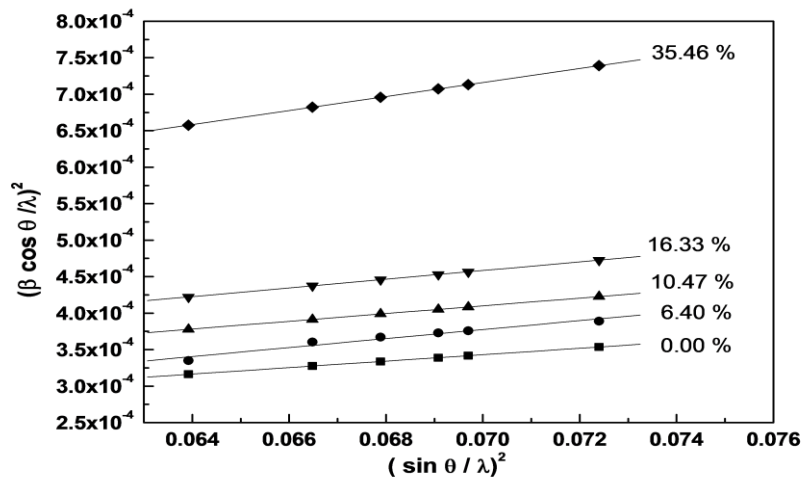


Fig. 5: Williamson-Hall plots of  $(\beta \cos \theta / \lambda)^2$  and  $(\sin \theta / \lambda)^2$  of Al-Mg alloys for different deformation percentage.

From the linear fitting of the W–H plots at different deformation degrees of the Al-Mg alloys (Figure5), it has been confirmed that the X-ray line broadening in polycrystalline material is due to the presence of crystallite size effect as well as microstrain effect. The slopes of the W–H plot represent average internal microstrain in the Al-Mg alloys while the inverse of the intercept at  $(\beta \cos\theta/\lambda)^2$  axis gives the crystallite size according to the relation (2).

The dependence values of the average crystallite size determined from W-H plot from the (111), (200), (220) and (311) reflections on the degree of deformation is depicted in Fig.(6), which shows an exponential decrease. The crystallite size is, by definition, measured in direction normal to the reflection plane, i.e., in the  $\langle 111 \rangle$  direction. A considerable decrease of the crystallite size was observed with a probable upper limit of about 500nm for a thickness reduction less than 10.47 %. Therefore, the observed decrease in the crystallite size may be interpreted in terms of a columnar grain growth. On the other hand, the microstrain exhibited a contrast behavior, i.e., increases gradually with increasing thickness reduction for lower deformation, as indicated in Fig.(7). This variation may be due to the increase of ordering (degree of preferred orientation) and the increase of the structural defects among which the grain boundary. Also, it was confirmed quantitatively by line profile analysis. Due to the high degree of preferred orientation only one order of reflection can be measured accurately enough.

### 3.2.2. Lattice parameters

From the XRD analysis of Al-Mg alloys should be the crystal structure is face centered cubic structure (fcc). It is confirmed by comparing the peak positions ( $2\theta$ ) of the XRD patterns as a function of deformation degrees with the standard PDF number 04-0787. The lattice constant 'a' for the cubic phase structure is determined by the relation;

$$a = d_{(hkl)} \sqrt{(h^2 + k^2 + l^2)} \quad (3)$$

The calculated values of lattice constants as a function of thickness reduction are showed in Fig.(8-a) and recorded in Table 2. It is can be seen that, the average value of lattice constant is 4.049 Å. In addition, the Nelson–Riley curve is plotted between the calculated 'a' for different planes and the error function [12];

$$f(\theta) = \frac{\cos^2 \theta}{2 \sin \theta} + \frac{\cos^2 \theta}{2\theta} \quad (4)$$

A typical Nelson–Riley plot for a Al-Mg alloys is shown in Fig. (8-b) and Table2. It is observed that, the corrected lattice parameters from the Nelson–Riley plots are estimated of 4.058Å. The change in lattice constant for the deformed Al-Mg alloy over the bulk clearly suggests that the deformed grains are strained [13].

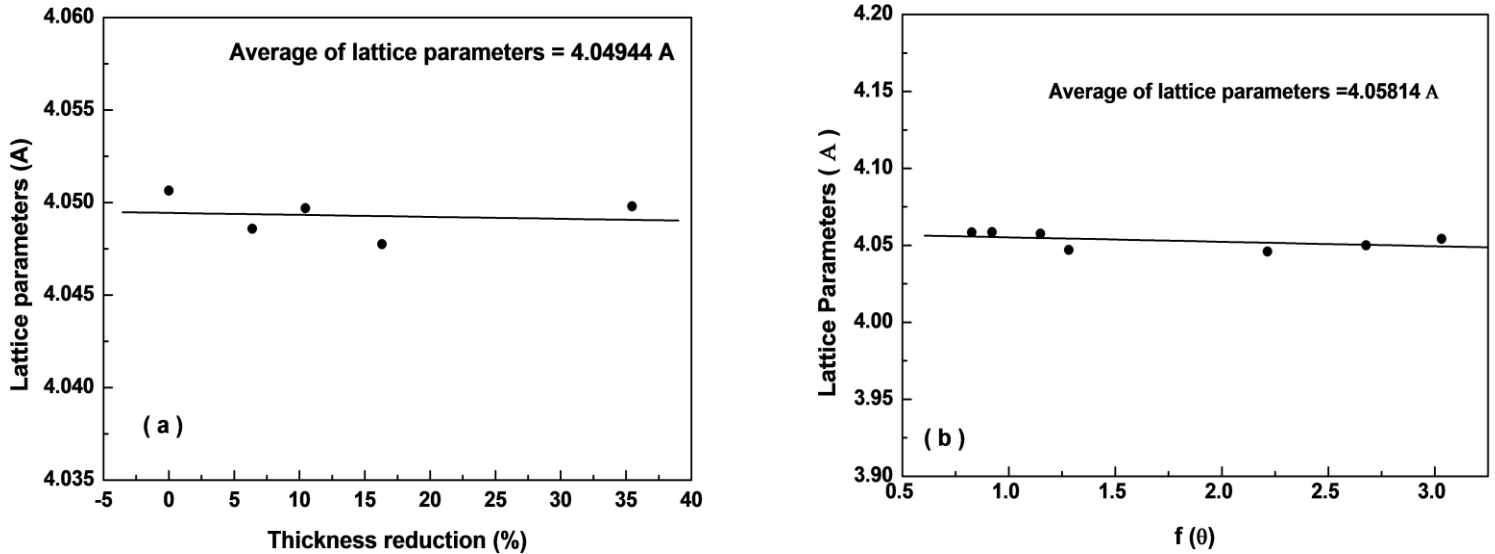


**Fig.8: variation of lattice parameters (a) as a function of thickness reduction (b) Nelson–Riley plot for an Al-Mg alloys.**

The principals of internal stress analysis by the X-ray diffraction is based on measuring angular lattice strain distributions. Residual internal stress is the stress that remains in the material after the external force that caused the stress has been removed. The total internal stress is consists of three types of stresses; they are thermal stress, mechanical stress and an intrinsic stress. Thermal stress depends on the thermal expansion coefficient, but intrinsic stress is due to the accumulating effect of the crystallographic flaws, these flaws are built in the Al-Mg alloys during compresses. On the other hand, mechanical stress is due to the deformation effect and elastic parameters of Al-Mg alloys. To get rid of the thermal stresses, samples were annealed at 773 K for 10 hr, which is found 5.00% of total stress. Therefore it is believed that for high melting material like Mg, the internal stress accumulates and tends to dominate over thermal stress. The average internal stress in the prepared samples is calculated by the following relation [14],

$$S = \frac{Y}{2\gamma} \left( \frac{a_o - a}{a_o} \right) \quad (5)$$

Where ( $Y$ ) and ( $\gamma$ ) are Young's modulus and Poisson's ratio of Al-Mg alloys, respectively.

The calculated values of ( $Y$ ) and ( $\gamma$ ) were found to be approximately equal 68.85 GPa and 0.33, respectively [15], while ( $a_0$ ) is the bulk lattice constant of Al-Mg alloys [Ref. PDF number 04-0787]. The estimated value of ( $a$ ) refers to the lattice constant which is perpendicular to the original plane. The origin of the internal stress is also related to the lattice misfits who is turn depend upon the deformation degrees. The calculated values of internal stress of Al-Mg alloys with various deformation degrees are given in Table 2 and Fig.(9). It is clear that, the values of internal stress ( $S$ ) are found to be in the range of  $(-1.74 \times 10^9)$  and  $(-2.49 \times 10^9)$  dy/cm<sup>2</sup>, the negative values indicate to a compressive state. Also, it is observed there the a linear relationship between the deformation degree and the absolute value of the internal stress, this is due to the lattice constant of prepared samples is greater than that of the slandered value while ( $Y$ ) and ( $\gamma$ ) are approximately unchanged. This is agreement with the reported results [5, 6].

### 3.2.4. Dislocation density

A dislocation density is defined as the length of dislocation lines per unit volume. This is due to an imperfection in a crystal associated with the misregistry of the lattice. Unlike vacancies and interstitial atoms, dislocations are not equilibrium imperfections, i.e. thermodynamic considerations are insufficient to account for their existence in the observed densities. In fact, the growth mechanism involving dislocation of a matter is important. The dislocation density has been estimated using Williamson and Smallman method using the relation [16,17].

$$\rho = \frac{15\varepsilon}{aD} \quad (6)$$

The calculated values of dislocation density for Al-Mg alloys as a function of deformation degree are recorded in Table 2 and shown in Fig.10.

**Table 2: microstructural parameters of Al-Mg alloys having a different deformation degree.**

Deformation degree (%)	$2\theta^\circ$	$d(\text{\AA})$	(hkl)	A calculated ( $\text{\AA}$ )	D(nm)	$S \times 10^9$ ( $\text{dy/cm}^2$ )	$\varepsilon \times 10^{-3}$	$\rho \times 10^{10}$ line/cm <sup>2</sup>
Zero%	38.500	2.338	(111)	4.0495	552	-1.742	5.19	3.48
	44.800	2.023	(200)	4.0460	546		5.21	3.54
	65.200	1.431	(220)	4.0475	534		5.28	3.66
	78.100	1.224	(311)	4.0596	528		5.32	3.72
6.40%	38.543	2.336	(111)	4.0461	514	-1.955	5.34	3.85
	44.828	2.022	(200)	4.0440	512		5.55	4.02
	65.234	1.430	(220)	4.0447	508		5.57	4.07
	78.112	1.224	(311)	4.0595	506		5.64	4.12
10.47%	38.521	2.337	(111)	4.0478	525	-2.245	5.64	3.98
	44.814	2.022	(200)	4.0440	514		5.75	4.15
	65.215	1.431	(220)	4.0475	507		5.78	4.23
	78.108	1.224	(311)	4.0595	494		5.82	4.35
16.33%	38.532	2.336	(111)	4.0461	498	-2.271	5.88	4.38
	44.834	2.022	(200)	4.0440	493		5.95	4.47
	65.223	1.430	(220)	4.0447	487		6.02	4.58
	78.143	1.223	(311)	4.0562	482		6.21	4.76
35.46%	38.511	2.338	(111)	4.0495	490	-2.489	7.66	5.79
	44.806	2.023	(200)	4.0460	486		7.71	5.88
	65.208	1.431	(220)	4.0475	475		7.75	6.05
	78.124	1.223	(311)	4.0562	552		8.09	6.18

It is observed that, with the increasing of the deformation degree there is a gradual increase in the dislocation density up to a deformation of 6.40 %, beyond it there is a slight increasing , after the deformation percentage of 16.33% there is a rapidly increasing of ( $\rho$ ), where it reach to a maximum value is  $5.88 \times 10^{10}$  line/cm<sup>2</sup> at 35.46%.



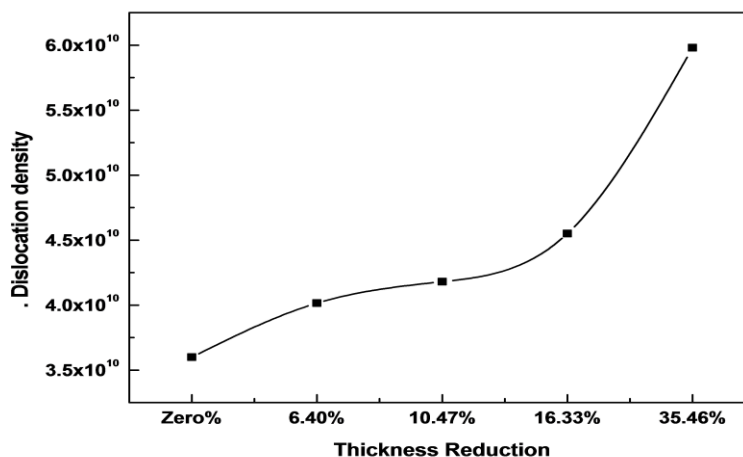


**Fig. 10: Variation of dislocation density of Al-Mg alloys as a function of thickness reduction.**

#### 4. Conclusion

X-ray diffraction line broadening analysis has been used for measuring the microstructure parameters of Al-Mg alloys as a function of plastic deformation degrees. From the preferred orientation studies, the degree of preferred orientation was found to be playing a dominant role over the microstructure parameters in Al-Mg alloys. The optimum crystallization of Al-Mg alloys was observed at the deformation percentage 10.47% ,and at higher thickness reduction the crystals agglomeration was often decomposed. The lattice constant, crystallite size, internal stress, microstrain and dislocation density were calculated. There is a progressive decreasing in the crystallite size and there was an increasing in microstrain and dislocation density with higher deformation percentage.

#### Acknowledgement

The authors sincerely thank Prof. Dr. **E.A.Badawi**, El-Minia University, Faculty of Science, Physics department for providing the Al-Mg alloys samples.

#### References

- [1] M. A. Abdel-Rahman, A.G. Attallah, M. El.sayed, A. A. Ibrahim, A.A. Akl , A.E.Ali and E.A.Badawi; Def.and Diff. Forum; Vols.337-338 (2013)11
- [2]L.K.Mansur; J. Nucl. Mater.,Vol. 216 (1994)97
- [3]M.Griffiths; J. Nucl. Mater., Vol. 159 (1988)190
- [4]P.K.Kalila,B.K.Sarma and H.L.Das; Bull. Mater. Sci., Vol. 23,No.4 (2000)313
- [5]N.Choudhury and B.K.Sarma; Bull. Mater. Sci., Vol. 32,No.1 (2009)43
- [6]K.Kapoor, D.Lahir, S.V.R.Rao, T.Sanyal and B.P.Kashyap; Bull. Mater. Sci., Vol. 27,No.1 (2004)59
- [7]Th. H. Keijser, D. I. De Langford, E. J. Mittemeijer and A.B.P.Vogels; *J. Appl. Cryst.* 15 (1982) 308
- [8]B.E. Warren ;*X-ray diffraction* (London: Addison Wesley Publishing Co.) (1969)18
- [9] R.L.Snyder and R.A. Young;TheRietveld Method, ed., Oxford University Press (1991)111
- [10] P. Rama Rao and T.R. Anantharaman;*Z. Metallk.* Vol. 54 (1963)658
- [11] J.V. Sharp, M.J. Makin andandJ.W.Christian;*Phys. StatusSolidi*; Vol.11 (1965) 845
- [12]J.B.Nelson andD.P.Riley; Proc. Phys. Soc. (London) Vol. 57(1945)160
- [13]K.Reichelt andX. Jiang ; *Thin Solid Films*; Vol. 91(1990) 191
- [14]K.L.Chopra ; *Thin film phenomena* (New York; McGraw Hill) (1969) 270
- [15] R.F.S. Hearman; *Physics of solid state* (eds) S Balakrishna,MK Krishnamurthi and B Ramachandra Rao (New York: Academic Press) (1969) 408
- [16] A. KropidLowska, J. ChojnaCki, A. Fahmi and B. Becker; Dalton Trans. 47 (2008) 6825
- [17] V. Bilgin, S. Kose, F. Atay and I. Akyuz; Mater. Chem. Phys. 94 (2005) 103, 07-309